FLOW BOILING IN MICROCHANNELS WITH HFE-7100: EXPERIMENTAL RESULTS AND COMPARISION WITH CORRELATIONS

Ali H. Al-Zaidi[1,2], Mohamed M. Mahmoud[3], Tassos G. Karayiannis[1*]

[1]Department of Mechanical and Aerospace Engineering, Brunel University London, Uxbridge, UB8 3PH, UK
[2]University of Misan, Al-Amarah, 62001, Iraq
[3]Faculty of Engineering, Zagazig University, Zagazig, 44519, Egypt

ABSTRACT

An experimental investigation of flow boiling heat transfer in a copper multi-microchannel heat sink with a hydraulic diameter of 0.46 mm is described in this paper. The heat sink consisted of 25 rectangular microchannels, which were 0.7 mm wide, 0.35 mm deep and 25 mm long. The separating wall thickness between the channels was 0.1 mm and the width of the heat sink was 20 mm giving a base area of 500 mm². HFE-7100 was chosen as the test fluid due to its environmentally friendly nature and high dielectric strength. It was also considered a suitable choice for cooling electronic components that require working surface temperature between 80 °C to 125 °C. A high-speed, high-resolution camera was used to capture the flow patterns during the experiments. All experiments were performed at a system pressure of 1 bar, inlet sub-cooling temperature of 5 K, mass flux ranging from 50 to 250 kg/m² s and a heat flux range of 43.96−335.29 kW/m². Four flow patterns were observed namely bubbly, slug, churn and annular flow. It was found that the local heat transfer coefficient increases with increasing heat flux and decreases slightly with increasing vapour quality, while there is a negligible effect of mass flux. The experimental results were compared with a number of existing heat transfer correlations that were proposed for macro and micro scale with some correlations showing good agreement. Similar comparisons with pressure drop correlations were also included.

KEY WORDS: Flow boiling, Flow patterns, Heat transfer coefficient, Pressure drop, Horizontal microchannel, Correlations.

1. INTRODUCTION

The rapid evolution of semiconductor technology led to a continuous demand on miniaturization and improvements of the performance of electronic devices. This means that high thermal power is generated from a small footprint area and thus the thermal management process in these devices is a big challenge. For example, Kadam and Kumar [1] mentioned that the heat flux in high power integrated circuits (ICs) and laser mirror could reach 1 MW/m², while it exceeds 10 MW/m² in the avionics and Very Large Scale Integrated Circuits (VLSIC). Karayiannis and Mahmoud [2] reported that, the average heat flux could reach 2 MW/m² in high performance computers and 4.5 MW/m² in desktop computers by 2026, while the heat flux in insulated gate bipolar transistor modules could be in the range 10−50 MW/m². Bachmann and Bar-Cohen [3] stated that the hot spots can be 6−10 times the chip average power, hence they can range between 12−20 MW/m² and 27−45 MW/m² in high performance computers and desktop computers, respectively [2]. As a result, several cooling techniques were investigated by many researchers with the aim of expanding the currently possible cooling capacity to meet the aforementioned high heat flux values. These techniques include heat pipes, single-phase liquid cooling, thermoelectric modules, immersion liquid cooling, vapour

*Corresponding Author: tassos.karayiannis@Brunel.ac.uk

compression refrigeration cycles and direct-liquid spray cooling. However, these techniques have technical limitations and an effective cooling technique is still required. Two-phase flow boiling in micro passages, as part of an integrated pump-driven system, is considered one of the most promising cooling solutions that can dissipate high heat fluxes. This technique is still not commercialized possibly due to the lack of understanding of several fundamental aspects such as the dominant heat transfer mechanism(s) [4-9], flow instability and its effect on heat transfer rates [10-11], the complex effect of parameters such as channel aspect ratio, surface characteristics, length of channels [12-14] on flow patterns and heat transfer rates and predictive correlations for pressure drop and heat transfer rates.

This study aims to investigate experimentally flow boiling heat transfer of HFE-7100 in a rectangular multi-microchannel heat sink. Twenty five microchannels with a hydraulic diameter of 0.46 mm were manufactured using a CNC machine. All experiments were conducted at a system pressure of 1 bar, sub-cooling temperature near 5 K, five different mass fluxes ranging from 50 to 250 kg/m^2 s and a heat flux range of 43.96−335.29 kW/m^2. Flow visualization was carried out using a high-resolution, high-speed camera integrated with a microscope, in order to capture the features of flow patterns during the experiments. The experimental results were used to evaluate some existing pressure drop and heat transfer correlations.

2. EXPERIMENTAL SYSTEM

The description of the experimental facility was presented in detail in Al-Zaidi et al. [15]. It consists of a liquid reservoir, sub-cooler, micro-gear pump, two Coriolis flow meters, pre-heater, test section, high-speed camera with a microscope and chiller system, and is shown in Fig. 1. A Phantom high-speed high-resolution camera with a frame rate of 1000 fps at 512×512 pixel resolution was mounted on a microscope fitted with LED lighting system. This visualization system was used to observe and record the flow patterns in the channels. All the measuring instruments, such as thermocouples, pressure transducers and flow meters, were connected to the National Instruments Data Acquisition System (DAQ). This data logger has a frequency of 1 kHz, i.e. it can record 1000 data per second. A computer with LabVIEW software was used to record all the measured data from the rig. The data were taken for 2 minutes, after steady state condition was reached, i.e. overall stability of the mass flux, pressures and temperatures, and the average value was used in all calculations. Fig. 2(a) shows the main parts of the test section, which consists of a cover plate, housing, heat sink block, cartridge heaters and bottom plate. The cover plate was made of a transparent polycarbonate, while a Polytetrafluoroethylene block was used to fabricate the housing and the bottom plate. The heat sink block was made of oxygen-free copper with height, width and length of 94.5, 26 and 51 mm, respectively. Twenty five microchannels were manufactured using a high-precision milling machine (Kern HSPC-2216). These channels were 0.7 mm wide, 0.35 mm deep and 25 mm long as shown in Fig. 2(b) with an average surface roughness of 0.304 μm. Zygo NewView 5000 surface profiler was used to measure this surface roughness. Twelve K-type thermocouples, with a calibration uncertainty of ±0.038−0.12K, were inserted into the heat sink block to measure the temperature distribution in the vertical direction (five thermocouples) and along the channels (four thermocouples distributed in two rows; two per row) as seen in Fig. 2(b). The thermocouples distribution formed a cross shape such that one thermocouple was common at the intersection point between the vertical and horizontal directions. Note that three thermocouples were inserted to a distance of 3 mm in the other side of the heat sink and are not shown in Fig. 2(b). These set of six thermocouples were used to assess the temperature distribution in the transverse direction. In Fig. 2(b), the two horizontal rows of thermocouples were used to make sure that there is minimum axial heat conduction in the heating block and the heat flows in the vertical direction, i.e. 1D heat conduction. Two T-type thermocouples were inserted into the inlet and outlet plena to measure the fluid temperature, with a calibration uncertainty of ±0.024K. Two pressure transducers and one differential pressure transducer were connected between the inlet/outlet plenum to measure the inlet/outlet pressure and the total pressure drop along the channels.
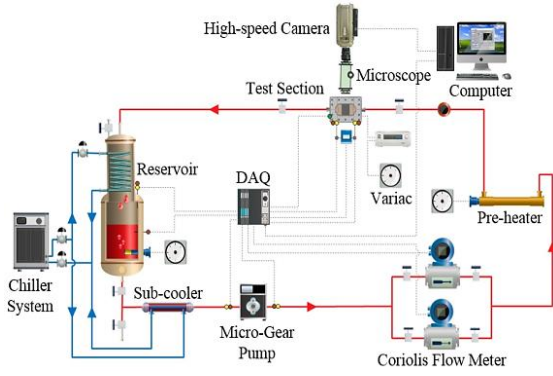
Fig. 1 Schematic diagram of the experimental facility.
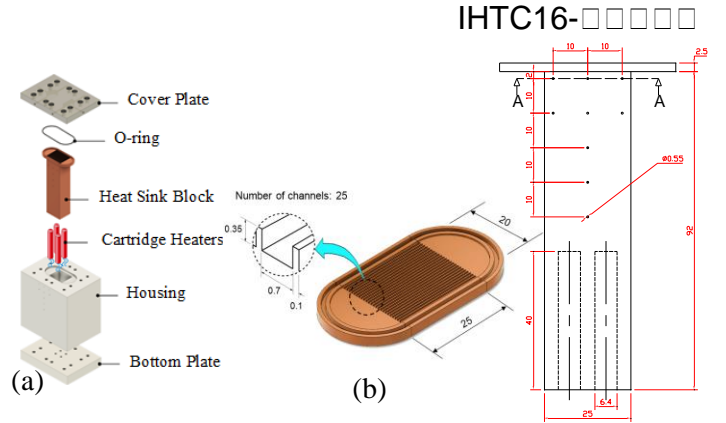
Fig. 2 Test section (a) exploded drawing (b) heat sink dimensions, in mm.

3. DATA REDUCTION

The experimental single-phase fanning friction factor is calculated from Eq. (1).

$$f_{exp} = \frac{\Delta P_{ch} * D_h}{2 L_{ch} * v_l * G_{ch}^2}$$
(1)

where ΔP_{ch}, D_h, L_{ch}, v_l and G_{ch} are the channel pressure drop, hydraulic diameter, channel length, liquid specific volume and channel mass flux, respectively. The hydraulic diameter is given by Eq. (2), while the channel pressure drop is found from Eq. (3).

$$D_h = 2 H_{ch} * W_{ch}/(H_{ch} + W_{ch})$$
(2)

$$\Delta P_{ch} = \Delta P_{meas} - (\Delta P_{ip} + \Delta P_{sc} + \Delta P_{se} + \Delta P_{op})$$
(3)

where H_{ch}, W_{ch}, ΔP_{meas}, ΔP_{ip}, ΔP_{sc}, ΔP_{se} and ΔP_{op} are the channel height, channel width, the total measured pressure drop along the channel, the pressure drop due to the change in flow direction by 90° in the inlet plenum, the sudden contraction pressure drop at the channel inlet, the sudden expansion pressure drop at the channel outlet and the pressure drop due to the change in flow direction by 90° in the outlet plenum, respectively. The value of each component is found from a procedure that was described in [16]. The local single-phase and two-phase heat transfer coefficient is calculated from Eq. (4) and (5), respectively.

$$h_{sp(z)} = \frac{q_b^{''} * (W_{ch} + W_{fin})}{(T_{wi(z)} - T_{f(z)}) * (W_{ch} + 2\eta * H_{ch})}$$
(4)

$$h_{tp(z)} = \frac{q_b^{''} * (W_{ch} + W_{fin})}{(T_{wi(z)} - T_{sat(z)}) * (W_{ch} + 2\eta * H_{ch})}$$
(5)

where $q_b^{''}$, W_{fin}, $T_{f(z)}$, $T_{wi(z)}$, $T_{sat(z)}$ and η are the base heat flux, the fin width, the local fluid temperature, local internal surface temperature, local saturation temperature and fin efficiency, respectively. The base heat flux and the local internal surface temperature can be found from Eq. (6) and (7), respectively. The local saturation temperature is found from the corresponding local pressure in the saturated zone with the assumption that the pressure drop varies linearly.

$$q_b^{''} = k_{cu} \frac{dT}{dy}$$
(6)

$$T_{wi(z)} = T_{th(z)} - \frac{q_b^{''} * Y}{k_{cu}}$$
(7)

where k_{cu} is the thermal conductivity of copper and $T_{th(z)}$ is the local thermocouple temperature. The vertical distance between the last thermocouple and the channel bottom, Y is 4.15 mm. The length of the single-phase region is found from Eq. (8).

$$L_{sub} = \frac{\dot{m} * cp_l (T_{sat(z,sub)} - T_{fi})}{q_b^{''} * W_b}$$
(8)

3

where $\dot{m}$, cp_l and T_{fi}, W_b are the mass flow rate, specific heat capacity, inlet fluid temperature and the base width, respectively. The local saturation temperature of the fluid at the end of the subcooled zone $T_{sat(z,sub)}$ is found from the local saturated pressure at subcooled zone $P_{sat(z,sub)}$ that is calculated as follows.

$$P_{sat(z,sub)} = P_i - \frac{2f * G_{ch}^2 * L_{sub*} v_l}{D_h}$$

(9)

where P_i is the inlet pressure. The experimental uncertainty values were calculated using the method given in [17]. All two-phase flow experiments were conducted at inlet sub-cooling temperature near 5 K and system pressure of 1 bar. The maximum uncertainty value for the friction factor, average Nusselt number, heat flux, mass flux, vapour quality and heat transfer coefficient are 2.05%, 6.47%, 6.88%, 0.64%, 10.2% and 13.48%, respectively.

4. RESULTS AND DISCUSSION

4.1 Single phase validation

Single-phase experiments were performed before conducting two-phase experiments to validate the experimental rig. Fig. 3 shows the experimental fanning friction factor versus Reynolds number, while the average Nusselt number versus Reynolds number was plotted in Fig. 4. The experimental results were compared with some existing correlations [18-21]. The figures indicate that, there is a good agreement between the experimental friction factor and the correlation by Shah and London [18] for fully developed flow and between the average Nusselt number and the equations proposed by [19] and [21] for developing laminar flow in a single channel, which confirms the system validation.
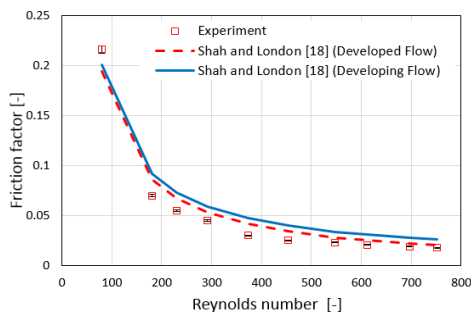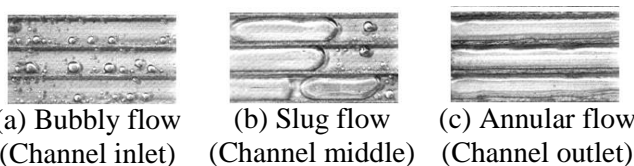

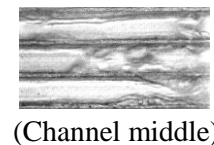**Fig. 3** Experimental Fanning friction factor versus Reynolds number.
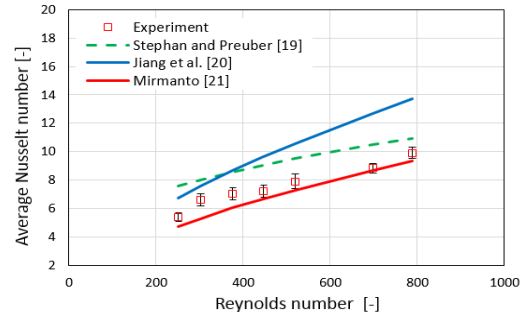
Fig. 4 Average Nusselt number versus Reynolds number.

4.2 Flow boiling patterns

The flow patterns presented in this paper were visualized at the heat sink centre near the channel inlet, near the middle and near the outlet. In this study, four flow patterns were observed, namely; bubbly, slug, churn and annular flow, see Fig. 5 and 6. As shown in Fig. 5(a), nucleation occurs at the channel corners. This was also found by [22-24]. Bubbly flow was observed near the inlet and is characterized by several small bubbles with size smaller than the channel width. Slug flow was observed near the middle with the features of a long cylindrical bubble followed by small bubbles, see Fig. 5(b). Annular flow is observed near the outlet and is characterized by a vapour core surrounded by a liquid film, see Fig. 5(c). When the heat flux was increased slightly to 63.087 kW/m^2, churn flow regime was observed near the middle with the characteristics of local distortions near the merging location of the elongated bubbles, see Fig. 6. Because this regime occurs over a narrow range of experimental conditions, it may be considered as a transition regime between slug and annular flow.


(a) Bubbly flow (Channel inlet) (b) Slug flow (Channel middle) (c) Annular flow (Channel outlet)

(Channel middle)

Fig. 5 Observed flow patterns at a heat flux of 51.078 kW/m^2 and mass flux of 50 kg/m^2 s.

Fig. 6 Churn flow at a heat flux of 63.087 kW/m^2 and mass flux of 50 kg/m^2 s.

4.3 Two-phase heat transfer

Fig. 7 illustrates the effect of heat flux on the local heat transfer coefficient at a mass flux of 250 kg/m^2 s. This figure shows that, when the heat flux increased, the local heat transfer coefficient also increased, which agrees with [24-28]. This figure was divided into two regions with respect to vapour quality; namely low and intermediate/high quality regions, in order to clarify the effect of heat flux. In the low quality region (x<0.1), the flow pattern was bubbly flow and the increase in the heat transfer coefficient with heat flux could be due to an increase in the bubble generation frequency. In the intermediate/high quality region (x>0.1) where the flow pattern was slug or annular flow, the increase in the heat transfer coefficient with heat flux could be due to the increase in the liquid film evaporation rate.
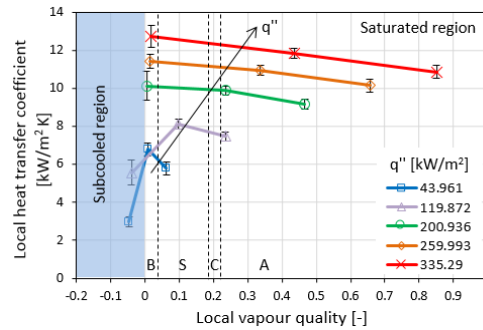
Fig. 7 Effect of heat flux at a mass flux of 250 kg/m^2 s, (B) bubbly (S) slug (C) churn (A) annular.

Fig. 7 shows the trend of the local heat transfer coefficient versus the local vapour quality at each heat flux. It can be seen that, at a given heat flux and low qualities (x<0.1) where the flow pattern was bubbly, the local heat transfer coefficient reached a peak value. This could be due to the evaporation process in the liquid micro layer underneath the nucleating bubbles. At high qualities (x>0.1), the local heat transfer coefficient decreased with increasing local vapour quality. Similar trend, decreasing heat transfer coefficient with increasing vapour quality, was also found by [6,29,30]. This reduction could be due to an increase in the wall superheat in the axial direction towards the channel exit. At a given heat flux, the local surface temperature increased towards the channel exit due to partial dry out and hence the wall superheat increased; higher surface-to-saturation temperature difference. This led to lower heat transfer coefficient.

Five different mass fluxes were tested ranging from 50 to 250 kg/m^2 s as illustrated in Fig. 8 in order to study the effect of mass flux. It seems that, there is no clear effect of mass flux on the local heat transfer coefficient in the range studied. This negligible effect was also reported in several past studies such as [26,31-34].
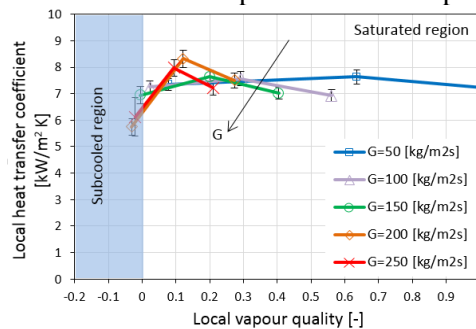
Fig. 8 Effect of mass flux at a heat flux of 100 kW/m^2.

The above results showed that the local heat transfer coefficient increases with heat flux and decreases with increasing local quality, while there is a negligible effect of mass flux. The main objective of this paper is to design a multi-microchannel heat sink that can be used for cooling electronic components. A small-scale thermal management system using a liquid pump cycle is proposed for this heat sink. In order to reduce the energy consumption by the pump, reduce the overall size and the system maintenance, the system pressure was kept near atmospheric pressure and low flow rates were tested, i.e. low Reynolds number. HFE-7100 was chosen as a working fluid due to its high dielectric strength and low global warming potential. The wall

temperature was maintained under 80 °C, while 335.29 kW/m^2 was dissipated from a base area of 500 mm^2 corresponding the hot chip area. The inlet sub-cooling temperature was controlled near 5 K and the maximum measured total pressure drop was 4 kPa. The measured energy consumption by the micro-gear pump at the highest heat flux value (335.29kW/m^2) was 14.25 W which means low pumping power. It is worth mentioning that, if the coefficient of performance (COP) is calculated, the value will be 11.8, which is much higher than miniature vapour compression systems, see [35]. Local heat transfer coefficient as high as 12,710 W/m^2 K was reached at a flow rate of 0.067 L/min. Although moderate heat fluxes were dissipated, it is possible to use flow boiling in micro passages for cooling electronics at very low flow rates and system pressure near one bar. The effect of channel aspect ratio is now to be examined to help design microchannels that can dissipate higher heat flux at these low pressure and low flow rate conditions.

4.4 Evaluation of existing correlations

Six existing heat transfer correlations [25,38-42] were evaluated as shown in Fig. 9. Eq. (10) and (11) were used to evaluate these existing correlations as follows:

$$\Theta = \frac{N_{pred}}{N_{exp}} * 100\%$$
(10)

$$MAE = \frac{1}{N}\sum \left|\frac{h_{pred}-h_{exp}}{h_{exp}}\right| * 100\%$$
(11)

where Θ, *MAE* and *N* are the percentage of data points predicted within ±30% error bands, the mean absolute error and the number of data points, respectively. Since the present heat sink is partly heated, i.e. channels are heated from three sides, a correction factor was used, see Eq. (12). This procedure was also adopted by [6,36,37].

$$HTC = \left(\frac{Nu_3}{Nu_4}\right) * h_{tp}$$
(12)

where h_{tp} is the two-phase heat transfer coefficient obtained from the correlation. Nu_3 and Nu_4 are Nusselt numbers for thermally developed laminar flow with three-sides and four-sides heated, respectively and are calculated from Eq. (13) and (14), [18].

$$Nu_3 = 8.235(1 - 1.833\beta + 3.767\beta^2 - 5.814\beta^3 + 5.361\beta^4 - 2\beta^5)$$
(13)

$$Nu_4 = 8.235(1 - 2.042\beta + 3.085\beta^2 - 2.477\beta^3 + 1.058\beta^4 - 0.186\beta^5)$$
(14)

The value Θ of and *MAE* for each of the comparison are included in Fig. 9. Lazarek and Black [25] and Kim and Mudawar [38] resulted in low Θ values and relatively high *MAE* values of 36.01% and 40.5%, respectively. The comparisons with the other correlations were reasonable and similar with a *MAE* value ranging within 14% and 21% and relatively high Θ values.

Fig. 10 depicts a comparison with some existing two-phase pressure drop correlations. This comparison shows that the correlation by Mishima and Hibiki [43] predicted the data very well with a *MAE* of 18.16%, while the correlations by Qu and Mudawar [44] and Li and Wu [45] predicted the results with less accuracy with a *MAE* of 36.5% and 93.95%, respectively.
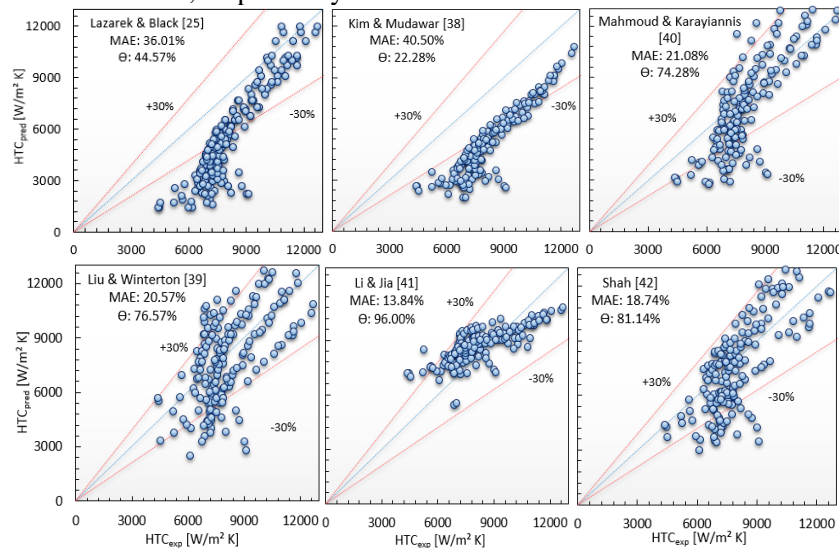
Fig. 9 Comparison with existing heat transfer correlations for macro/microchannel.
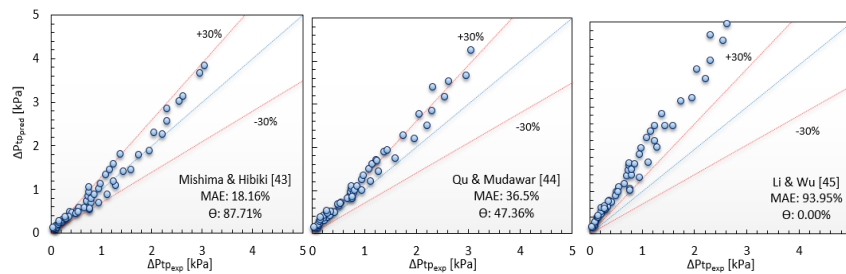
Fig. 10 Comparison with existing two-phase pressure drop correlations.

5. CONCLUSIONS

Flow visualization, heat transfer and pressure drop experiments were performed in multi-microchannels with a hydraulic diameter of 0.46 mm. HFE-7100 was tested at inlet sub-cooling of 5 K, system pressure of 1 bar, heat flux of 43.96−335.29 kW/m^2 and mass flux of 50−250 kg/m^2 s. The main conclusions are:

1. Bubbly, slug, churn and annular flow were observed.
2. The local heat transfer coefficient increases with heat flux and decreases with increasing local vapour quality, while there is no clear effect of mass flux in the range studied and with this fluid.
3. The heat transfer correlations by Li and Jia [41] and Shah [42] predicted the results well with a MAE of 13.84% and 18.74%, respectively. The correlations by Liu and Winterton [39] and Mahmoud and Karayiannis [40] also gave very reasonable predictions.
4. The pressure drop correlation by Mishima and Hibiki [43] predicted the results with a MAE of 18.16%.
5. In this study, a base heat flux as high as 335.29 kW/m^2 was dissipated from a base area of 500 mm^2. The working surface temperature was kept under 80 °C at a system pressure near the atmospheric pressure. The maximum measured total pressure drop was 4 kPa with a flow rate of 0.067 L/min. This means low pumping power, approximately 14 W, needed to deliver such vales. As shown in this study, it is possible to use flow boiling in micro passages for cooling electronics at very low flow rates and system pressure near one bar. Further studies are underway to increase the upper limit of heat flux by varying the channel aspect ratio and modifying the channel surface micro structure.

ACKNOWLEDGMENT

REFERENCES

[1] Kadam, S. T., Kumar, R., "Twenty first century cooling solution: Microchannel heat sinks," *Int. J. Therm. Sci.*, 85, pp. 73–92, (2014).
[2] Karayiannis, T. G., Mahmoud, M. M., "Flow boiling in microchannels: Fundamentals and applications," *Appl. Therm. Eng.*, 115, pp. 1372–1397, (2017).
[3] Bachmann, C., Bar-Cohen, A., "Hotspot remediation with anisotropic thermal interface materials," *in 11th IEEE Intersociety Conference on Thermal and Thermomechanical Phenomena in Electronic Systems*, pp. 238–247, (2008).
[4] Hamdar, M., Zoughaib, A., Clodic, D., "Flow boiling heat transfer and pressure drop of pure HFC-152a in a horizontal mini-channel," *Int. J. Refrig.*, 33, pp. 566–577, (2010).
[5] Anwar, Z., Palm, B., Khodabandeh, R., "Flow boiling heat transfer and dryout characteristics of R152a in a vertical mini-channel," *Exp. Therm. Fluid Sci.*, 53, pp. 207–217, (2014).
[6] Qu, W., Mudawar, I., "Flow boiling heat transfer in two-phase micro-channel heat sinks-I. Experimental investigation and assessment of correlation methods," *Int. J. Heat Mass Transf.*, 46, pp. 2755–2771, (2003).
[7] Mortada, S., Zoughaib, A., Arzano-Daurelle, C., Clodic, D., "Boiling heat transfer and pressure drop of R-134a and R-1234yf in minichannels for low mass fluxes," *Int. J. Refrig.*, 35, pp. 962–973, (2012).
[8] McNeil, D. A., Raeisi, A. H., Kew, P. A., Hamed, R. S., "Flow boiling heat-transfer in micro to macro transition flows," *Int. J. Heat Mass Transf.*, 65, pp. 289–307, (2013).
[9] Kuznetsov, V. V., Shamirzaev, A. S., Kozulin, I. A., Kozlov, S. P., "Correlation of the flow pattern and flow boiling heat transfer in microchannels," *Heat Transf. Eng.*, 34, pp. 235–245, (2013).
[10] Consolini, L., Thome, J. R., "Micro-channel flow boiling heat transfer of R-134a, R-236fa, and R-245fa," *Microfluid. Nanofluidics*, 6, pp. 731–746, (2009).
[11] Ohta, H., Inoue, K., Ando, M., Watanabe, K., "Experimental investigation on observed scattering in heat transfer characteristics for flow boiling in a small diameter tube," *Heat Transf. Eng.*, 30, pp. 19–27, (2009).

[12] Mahmoud, M. M., Karayiannis, T. G., Kenning, D. B. R., "Surface effects in flow boiling of R134a in microtubes," *Int. J. Heat Mass Transf.*, 54, pp. 3334–3346, (2011).

[13] Karayiannis, T. G., Mahmoud, M. M., Kenning, D. B. R., "A study of discrepancies in flow boiling results in small to microdiameter metallic tubes," *Exp. Therm. Fluid Sci.*, 36, pp. 126–142, (2012).

[14] Markal, B., Aydin, O., Avci, M., "Effect of aspect ratio on saturated flow boiling in microchannels," *Int. J. Heat Mass Transf.*, 93, pp. 130–143, (2016).

[15] Al-Zaidi, A. H., Mahmoud, M. M., Karayiannis, T. G., "Condensation Flow Patterns and Heat Transfer in Horizontal Microchannels," *Exp. Therm. Fluid Sci.*, 90, pp. 153–173, (2017).

[16] Remsburg, R., *Thermal design of electronic equipment*. CRC Press LLC, (2001).

[17] Coleman, H. W. and Steele, W. G., *Experimentation and uncertainty analysis for engineers*, 3nd ed. New York: Wiley, Chichester, (2009).

[18] Shah, R. K. and London, A. L, *Laminar flow forced convection in ducts, Supplement 1 to Advances in Heat Transfer*. Academic Press New York, (1978).

[19] Stephan, K., Preuber, P., "Warmeubergang und Maximale Warmestromdichte Beim Behaltersieden Binarer und Ternarer Flussigkeitsgemische," *Chem. Ing. Tech.*, 51, pp. 37, (1979).

[20] Jiang, P. X., Fan, M. H., Si, G. S., Ren, Z. P., "Thermal Hydraulic Performance of Small Scale Micro-Channel and Porous-Media Heat Exchangers," *Int. J. Heat Mass Transf.*, 44, pp. 1039–1051, (2001).

[21] Mirmanto, M., *Single-phase flow and flow boiling of water in horizontal rectangular microchannels*, Ph.D. Thesis, Brunel University London, (2013).

[22] Liu, D., Lee, P. S., Garimella, S. V., "Prediction of the onset of nucleate boiling in microchannel flow," *Int. J. Heat Mass Transf.*, 48, pp. 5134–5149, (2005).

[23] Soupremanien, U., Le Person, S., Favre-Marinet, M., Bultel, Y., "Influence of the aspect ratio on boiling flows in rectangular mini-channels," *Exp. Therm. Fluid Sci.*, 35, pp. 797–809, (2011).

[24] Fayyadh, E. M., Mahmoud, M. M., Sefiane, K., Karayiannis, T. G., "Flow boiling heat transfer of R134a in multi microchannels," *Int. J. Heat Mass Transf.*, 110, pp. 422–436, (2017).

[25] Lazarek, G. M. Black, S. H., "Evaporative heat transfer, pressure drop and critical heat flux in a small vertical tube with R-113," *Int. J. Heat Mass Transf.*, 25, pp. 945–960, (1982).

[26] Bao, Z. Y., Fletcher, D. F., Haynes, B. S., "Flow boiling heat transfer of Freon R11 and HCFC123 in narrow passages," *Int. J. Heat Mass Transf.*, 43, pp. 3347–3358, (2000).

[27] Sobierska, E., Kulenovic, R., Mertz, R., Groll, M., "Experimental results of flow boiling of water in a vertical microchannel," *Exp. Therm. Fluid Sci.*, 31, pp. 111–119, (2006).

[28] Özdemir, M. R., Mahmoud, M. M., Karayiannis, T. G., "Flow Boiling Heat Transfer in a Rectangular Copper," *J. Therm. Eng., Yildiz Tech. Univ. Press*, 2, pp. 761–773, (2016).

[29] Wang, Y. Sefiane, K., "Effects of heat flux, vapour quality, channel hydraulic diameter on flow boiling heat transfer in variable aspect ratio micro-channels using transparent heating," *Int. J. Heat Mass Transf.*, 55, pp. 2235–2243, (2012).

[30] Mirmanto, M., "Local pressure measurements and heat transfer coefficients of flow boiling in a rectangular microchannel," *Heat Mass Transf.*, 52, pp. 73–83, (2016).

[31] Pettersen, J., "Flow vaporization of CO2 in microchannel tubes," *Exp. Therm. Fluid Sci.*, 28, pp. 111–121, (2004).

[32] Oh, H. K., Son, C. H., "Flow boiling heat transfer and pressure drop characteristics of CO2 in horizontal tube of 4.57-mm inner diameter," *Appl. Therm. Eng.*, 31, pp. 163–172, (2011).

[33] Lim, T. W., You, S. S., Choi, J. H., Kim, H. S., "Experimental Investigation of Heat Transfer in Two-phase Flow Boiling," *Exp. Heat Transf.*, 28, pp. 23–36, (2015).

[34] Al-Gaheeshi, A. M., Mahmoud, M. M., Karayiannis, T. G., "Flow boiling heat transfer in a vertical small-diameter tube: Effect of different fluids and surface characteristics," *Proc. of the 4th International Forum on Heat Transfer*, pp. 1–9, (2016).

[35] Yuan, W., Yang, B., Yang, Y., Ren, K., Xu, J., Liao, Y., "Development and experimental study of the characteristics of a prototype miniature vapor compression refrigerator," *Appl. Energy*, 143, pp. 47–57, (2015).

[36] Kim, S. M., Mudawar, I., "Review of databases and predictive methods for heat transfer in condensing and boiling mini/micro-channel flows," *Int. J. Heat Mass Transf.*, 77, pp. 627–652, (2014).

[37] Wang, S., Bi, X., Wang, S., "Boiling heat transfer in small rectangular channels at low Reynolds number and mass flux," *Exp. Therm. Fluid Sci.*, 77, pp. 234–245, (2016).

[38] Kim, S. M., Mudawar, I., "Universal approach to predicting saturated flow boiling heat transfer in mini/micro-channels – Part II. Two-phase heat transfer coefficient," *Int. J. Heat Mass Transf.*, 64, pp. 1239–1256, (2013).

[39] Liu, Z., Winterton, R. H. S., "A general correlation for saturated and subcooled flow boiling in tubes and annuli, based on a nucleate pool boiling equation," *Int. J. Heat Mass Transf.*, 34, pp. 2759–2766, (1991).

[40] Mahmoud, M. M., Karayiannis, T. G., "Heat transfer correlation for flow boiling in small to micro tubes," *Int. J. Heat Mass Transf.*, 66, pp. 553–574, (2013).

[41] Li, X., Jia, L., "The investigation on flow boiling heat transfer of R134a in micro-channels," *J. Therm. Sci.*, 24, pp. 452–462, (2015).

[42] Shah, M. M., "Unified correlation for heat transfer during boiling in plain mini/micro and conventional channels," *Int. J. Refrig.*, 74, pp. 606–626, (2017).

[43] Mishima, K., Hibiki, T., "Some characteristics of air-water two-phase flow in small diameter vertical tubes," *Int. J. Multiph. Flow*, 22, pp. 703–712, (1996).

[44] Qu, W., Mudawar, I., "Measurement and prediction of pressure drop in two-phase micro-channel heat sinks," *Int. J. Heat Mass Transf.*, 46, pp. 2737–2753, (2003).

[45] Li, W., Wu, Z., "A general correlation for adiabatic two-phase pressure drop in micro/mini-channels," *Int. J. Heat Mass Transf.*, 53, pp. 2732–2739, (2010).